Synthesis of 3-Benzo[*b*]thienyl 3-Thienyl Ether via an Addition–Elimination Reaction and Its Transformation to an Oxygen-Fused Dithiophene Skeleton: Synthesis and Properties of Benzodithienofuran and Its π-Extended Derivatives

Koichi Mitsudo,*,† Yuji Kurimoto,† Hiroki Mandai,† and Seiji Suga*,†,‡

†Division of Applied Chemistry, Graduate School of Natural Science and Technology, Okayama University, 3-1-1 Tsushima-naka, Kita-ku, Okayama 700-8530, Japan

‡Research Center of New Functional Materials for Energy Production, Storage and Transport, Okayama University, 3-1-1 Tsushima-naka, Kita-ku, Okayama 700-8530, Japan

Supporting Information Placeholder

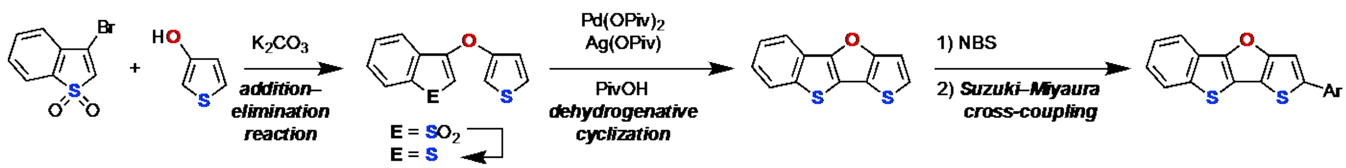

ABSTRACT: The synthesis of 3-benzo[*b*]thienyl 3-thienyl ether and its dehydrogenative cyclization leading to benzodithienofuran (BDTF; [1]benzothieno[3,2-*b*]thieno[2,3-*d*]furan) are described for the first time. Further transformation of BDTF to more π-extended BDTF derivatives and their fundamental physical properties are also studied.

Heteroatom-fused 2,2′-dithiophene skeletons, such as dithieno[3,2-*b*:2′,3′-*d*]thiophenes (DTTs), dithieno[3,2-*b*:2′,3′-*d*]pyrroles (DTPs), silolo[3,2-*b*:4,5-*b*′]dithiophene (dithienosiloles, DTSs), and phospholo[3,2-*b*:4,5′-*b*′]dithiophene, have received considerable attention as organic materials, and there have been several reports on the synthesis and application of these compounds.[1] In contrast, there have been only two reports on the synthesis of dithieno[3,2-*b*:2′,3′-*d*]furans (DTFs).[2]

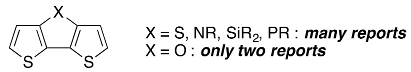

Karminski-Zamola and co-workers reported the first synthesis of a DTF derivative (Scheme 1).[2a] They converted furylacrylic acid to a DTF derivative through several steps including a Vilsmeier–Haak reaction and Knoevenagel condensation. Svoboda achieved the second synthesis of DTF derivatives from 3,4-dibromofuran via a Vilsmeier–Haak reaction and subsequent reaction with methyl thioglycolate, and decarboxylation.[2b] In their works, they constructed DTF skeletons by the cyclization reactions near a furan skeleton. However, it is difficult to apply such strategies for the synthesis of more π-expanded ladder-type DTFs. Indeed, to the best of our knowledge, there has been no report on the synthesis of such π-expanded DTF derivatives even for benzodithienofuran ([1]benzothieno[3,2-*b*]thieno[2,3-*d*]furan; BDTF) in spite of their promising properties as organic materials. In contrast, there have been several reports on the synthesis of π-expanded ladder-type DTTs such as BDTT ([1]benzothieno[3,2-*b*]thieno[2,3-*d*]thiophene).[3] In particular, Marks and co-workers recently reported excellent results regarding the synthesis of π-extended BDTT derivatives and their application to organic field effect transistors.[3b,3f]

Scheme 1. Previous Reports on the Synthesis of DTF Skeletons and Their Analogs

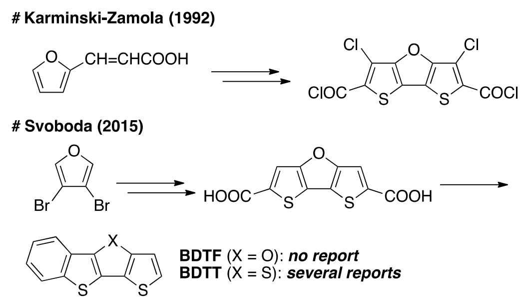

Our recent interest in the synthesis and properties of novel ladder-type thienoacenes[4] prompted us to investigate an efficient and general method for the synthesis of BDTF. A designed route for the construction of BDTF from 3-benzo[*b*]thienyl 3-thienyl ether is depicted in Scheme 2. We considered that BDTF **1** could be derived from precursor **2a** (X = Br) or **2b** (X = H) by a Pd-catalyzed cyclization reaction,[5] and precursor **2a** and **2b** could be prepared by a cross-coupling reaction (route A) or an addition–elimination reaction (route B). Although this approach should provide a straightforward access to DTF derivatives, there has been no previous report based on this schematic design. In fact, there has been only one report on the synthesis of a 3,3′-dithienyl ether derivative, in which 2,2′-positions are protected and could not be used for this approach.[6] We report here the first synthesis of a 3,3′-dithienyl ether derivative **2b** and Pd-catalyzed dehydrogenative cyclization for its transformation to BDTF **1**. Further π-extension of **1** and the physical properties of thus-obtained BDTF derivatives were also studied.

Scheme 2. Designed Strategy for the Construction of BDTF

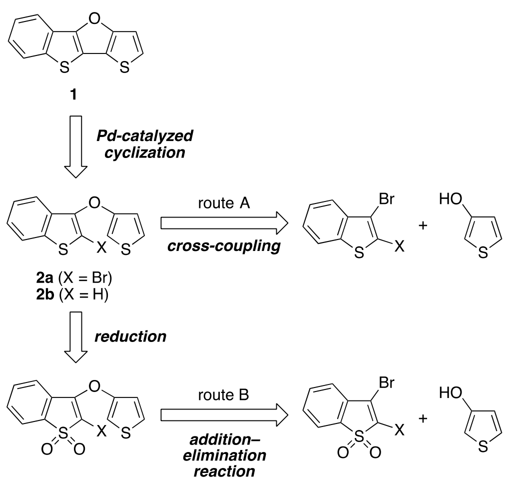

First, we attempted the synthesis of dithienyl ether derivatives by Pd- or Cu-catalyzed cross-coupling reactions between 3-bromobenzo[*b*]thiophene and 3-hydroxythiophene (Scheme 2, route A). Even though a variety of reaction conditions were examined, the desired dithienyl ethers could not be obtained at all, probably because tautomerization of 3-hydroxythiophene would be problematic (Scheme 3). 3-Hydroxythiophene is known to tautomerize to a keto tautomer (thiophen-3(*2H*)-one), and dimerization proceeds between them (Scheme 3).[7] While such dimerized compounds were not observed in the above reactions, we assumed that tautomerization would make this compound less nucleophilic so that the reaction would not proceed. Therefore, we changed our strategy from cross-coupling reactions to addition–elimination reactions using 3-hydoxythiophene (Scheme 2, route B).

Scheme 3. Tautomerization and Dimerization of 3-Hydroxythiophene

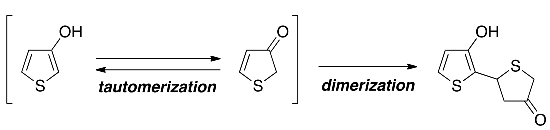

Addition–elimination reaction of 2,3-dibromobenzo[*b*]thiophene or 3-bromobenzo[*b*]thiophene with 3-hydroxythiophene did not proceed, probably due to the aromaticity of the thiophene ring. Therefore, we next selected 2,3-dibromobenzo[*b*]thiophene 1,1-dioxide (**3a**), which is much more electrophilic (Table 1).[8] In DMF, **3a** (0.2 mmol) was treated with 3-hydroxythiophene (**4**), derived from 3-thienylboronic acid (2.0 equiv) by oxidation using H_2O_2, in the presence of DABCO or Et_3N as a base (1.5 equiv), but the desired addition–elimination reaction did not proceed (entries 1 and 2). In contrast, with K_2CO_3, the addition–elimination reaction proceeded smoothly, and 3-(thiophen-3-yloxy)benzo[*b*]thiophene 1,1-dioxide (**5b**), a debrominated product, was unexpectedly obtained selectively in 79% yield (entry 3). The reaction was finished within 12 h (entry 4). It is not yet clear why the debromination proceeded. **5b** was also obtained from the addition–elimination reaction of 3-bromobenzo[*b*]thiophene 1,1-dioxide (**3b**) with **4** (entry 5, 75% yield). An advantage of these reactions is that they can be easily scaled-up (entry 3, 5.0 mmol scale, 75% yield; entry 5, 15 mmol scale, 74% yield). Thus-obtained **5b** was readily reduced to **2b** by treatment with DIBAL-H, as illustrated in Scheme 4 (96% yield).

Table 1. Optimization of Addition–Elimination Reaction for the Construction of 5[a]

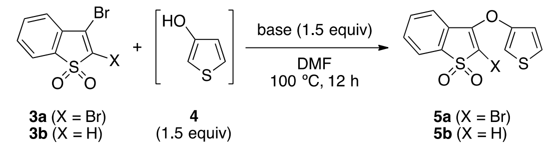

entry	3	base	time (h)	**5a** (%)[b]	**5b** (%)[b]
1	**3a**	DABCO	24	N.D.[c]	N.D.
2	**3a**	Et_3N	24	N.D.	N.D.
3	**3a**	K_2CO_3	24	N.D.	79 (75)[d]
4	**3a**	K_2CO_3	12	N.D.	74
5	**3b**	K_2CO_3	12	N.D.	75 (74)[e]

[a] Reaction conditions: **3a** or **3b** (0.20 mmol), base (1.5 equiv), DMF (1.0 mL) at 90 ºC. 3-Hydroxythiophene (**4**) was generated by the reaction of 3-thienylboronic acid and H_2O_2 aq, and used without purification.[9] [b] Isolated yield. [c] Not detected. [d] Performed with 5.0 mmol of **3a**. [e] Performed with 15 mmol of **3b**.

Scheme 4. Synthesis of 3-(3-Thienyloxy)benzo[*b*]thiophene (2b) by Reduction with DIBAL-H

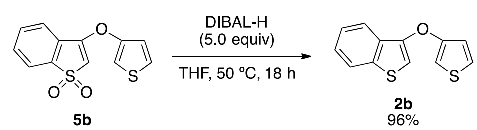

We next investigated transformations of **2b** to BDTF **1**. Screening of the reactions conditions revealed that Pd-catalyzed dehydrogenative cyclizations were effective for the construction of **1** (Table 2). In the presence of palladium pivalate ($Pd(OPiv)_2$, 10 mol %), AgOPiv (3.0 equiv), the dehydrogenative cyclization of **2b** proceeded to give the desired BDTF **1** in 77% yield (entry 1).[10] The efficiency of the reaction on a 2.0 mmol scale was similar to that on a 0.2 mmol scale (entry 2). The palladium catalyst and the silver salt play key roles in the reaction,[11] and only a trace amount of **1** was obtained in the absence of either $Pd(OPiv)_2$ or AgOPiv (entries 3 and 4). The use of a bulkier silver salt such as silver adamantane-1-carboxylate (AgOCOAd) gave a result similar to that with the use of AgOPiv (76%, entry 5). When NaOCOAd was used instead of a silver salt, the yield of **1** drastically decreased to 16% (entry 6). The yield of **1** also decreased to 65% when the reaction was performed at 160 ºC (entry 7). When DMF was used instead of pivalic acid (PivOH) at 160 ºC, the yield of **1** decreased to 49% (entry 8).

Table 2. Optimization of the Reaction Conditions for the Pd-Catalyzed Dehydrogenative Cyclization of 2b[a]

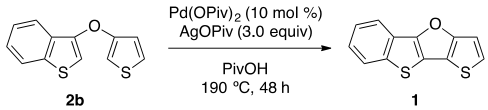

entry	deviation from standard conditions	yield (%)[b]
1	none	77
2	2.0 mmol of **2b** instead of 0.2 mmol	79
3	no $Pd(OPiv)_2$	<5
4	no AgOPiv	<5
5	AgOCOAd instead of AgOPiv	76
6	NaOCOAd instead of AgOPiv	16
7	performed at 160 ºC	65
8	DMF instead of PivOH at 160 ºC	49

[a] Reaction conditions: **2b** (0.20 mmol), $Pd(OPiv)_2$ (10 mol %), AgOPiv (3.0 equiv), PivOH (1.0 mL) at 190 ºC, 48 h. [b] Isolated yields.

Thus-obtained BDTF **1** was easily transformed to π-extended BDTF derivatives by a bromination reaction and subsequent Suzuki–Miyaura cross-coupling (Table 3). The bromination of **1** with NBS (1.1 equiv) proceeded smoothly at 25 ºC to give brominated BDTF **6**, and π-extended BDTFs **7** were obtained by Suzuki–Miyaura cross-coupling between **6** and arylboronic acids. For instance, in the presence of Pd[P(*t*-Bu)$_3$]$_2$ (5 mol %) and NaOH aq (1.0 M, 2 equiv), the reaction between **1** and phenylboronic acid gave 2-phenyl-BDTF **7a** in 89% yield (over 2 steps, based on **1**, entry 1). The yield of **7a** was 83% from 1.0 mmol of **1**. A variety of π-extended BDTFs **7** were obtained under similar conditions. Both an electron-rich arylboronic acid such as 4-tolylboronic acid and an electron-deficient arylboronic acid such as 4-cyanoboronic acid could be used to give coupling products **7b** and **7c** in respective yields of 93% and 81% (entries 2 and 3). More π-extended BDTF derivatives **7d–f** were also obtained by Suzuki–Miyaura cross-coupling using the corresponding arylboronic acids (entries 4–6). This strategy could also be used for the synthesis of a heteroaryl-substituted BDTF to afford 3-thienyl-BDTF **7g** in 84% yield (entry 7).

We next investigated the fundamental physical properties of BDTFs. First, UV–Vis absorption spectra were measured (Figure 1). The wavelength of maximum absorbance (λ_{max}) of **1** was at 311 nm and the onset value of absorbance (λ_{onset}) was 335 nm. The introduction of an aryl group highly influenced absorption, and λ_{onset} of **7a–g** were around 385–427 nm. In particular, **7c** which has a 4-cyanophenyl group had the longest λ_{onset} value (427 nm). These results suggest that the HOMO–LUMO gaps of **7a–g** are smaller than that of **1** due to π-extension, and that of **7c** is the smallest among them. A similar tendency was observed in TD-DFT calculations, where the energy gaps calculated at the B3LYP/6-31G(d) level were 4.06 eV (**1**), 3.19 eV (**7c**), and 3.30–3.79 eV (**7a**, **7b**, and **7d–g**), respectively.[12]

Table 3. Synthesis of π-Extended BDTF 7 by Bromination and Subsequent Suzuki–Miyaura Cross-Coupling [a]

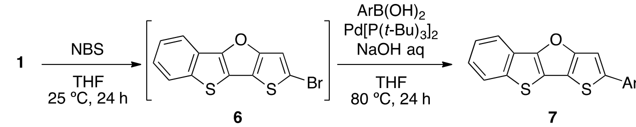

entry	Ar	7	yield (%)[b]
1	Ph	**7a**	89 (83)[c]
2	4-Me-C_6H_4	**7b**	93
3	4-CN-C_6H_4	**7c**	81
4	4-Ph-C_6H_4	**7d**	78
5	1-Np[d]	**7e**	87
6	2-Np	**7f**	92
7	3-thienyl	**7g**	84

[a] Reaction conditions: **1** (0.20 mmol), NBS (1.1 equiv) in THF (2 mL) at 25 ºC, 24 h, and then $ArB(OH)_2$ (1.5 equiv), Pd[P(*t*-Bu)$_3$]$_2$ (5 mol %), 1.0 M NaOH aq (2.0 equiv) at 80 ºC, 24 h. [b] Isolated yield over two steps based on **1**. [c] Performed with 1.0 mmol of **1**. [d] Np = naphthyl.

Figure 1. UV–Vis absorption spectra of **1** and **7a–g** measured in *o*-$C_6H_4Cl_2$ (1.0×10^{-5} M).

Next, cyclic voltammetry (CV) was carried out for **1** and **7a–g**.[13] In the cyclic voltammogram of **1**, an irreversible oxidation peak was observed at around 0.87 V (vs. Fc/Fc^+). The onset value of the oxidation peak was 0.74 V, which was similar to the reported oxidation potential of BDTT (0.73 V).[3f] In contrast to the results for **1**, reversible oxidation peaks were observed in the cyclic voltammograms of **7a–g**. These results suggest that the cationic species generated from **7a–g** under electro-oxidative conditions are more stable than that from **1** due to protection of the α-position of the thiophene unit.

The combined electrochemical and optical data and estimated HOMO–LUMO levels for **1** and **7a–g** are shown in Table 4. The value of E_{HOMO} for **7a** (–5.44 eV) was slightly higher than that for **1** (–5.54 eV) due to π-extension. A similar tendency was observed for **7b–g,** except for **7c** (–5.58 eV), which has an electron-withdrawing group. In contrast, the E_{LUMO} values for **7a–g** were all lower than that of **1**. These tendencies are consistent with the results of DFT calculations.[12]

Table 4. Electrochemical and Optical Data for BDTFs[a]

BDTF	λ_{max} (nm)	log ε	$\lambda_{onset}/E_g^{opt}$ (nm/eV)	E_{HOMO} (eV)	E_{LUMO} (eV)
1	311	4.57	335, 3.70	–5.54	–1.84
7a	356	4.58	391, 3.17	–5.44	–2.27
7b	357	4.83	392, 3.16	–5.37	–2.21
7c	385	4.57	427, 2.90	–5.58	–2.68
7d	372	4.73	412, 3.01	–5.42	–2.41
7e	350	4.24	401, 3.09	–5.47	–2.38
7f	372	4.89	409, 3.03	–5.36	–2.33
7g	353	4.71	385, 3.22	–5.40	–2.18

[a] E_{onset} values were determined by the onset of CV in CH_2Cl_2. All potentials were calibrated with reference to Fc/Fc^+. E_{HOMO} values were determined with reference to ferrocene (4.8 eV vs vacuum).[14] Optical band gap: $E_g^{opt} = 1240/\lambda_{onset}$. $E_{LUMO} = E_{HOMO} + E_g^{opt}$.

In conclusion, we have achieved the syntheses of dithienyl ether derivative **2b** by a addition–elimination reaction of 2,3-dibromobenzo[*b*]thiophene dioxide (**3a**) or 3-bromobenzo[*b*]thiophene dioxide (**3b**) with 3-hydroxythiophene (**4**). An efficient transformation from **2b** to BDTF **1** by Pd-catalyzed dehydrogenative cyclization was also developed. BDTF **1** could be readily transformed to π-extended BDTF derivatives **7a–g**. The fundamental physical properties of the BDTF derivatives were also studied. Further investigations of these derivatives are in progress in our laboratory.

ASSOCIATED CONTENT

Supporting Information

The Supporting Information is available free of charge on the ACS Publication website at :DOI: 10.1021/.

Experimental details, photophysical and electrochemical properties of **1** and **7a–g**, spectral data for all new compounds, data of theoretical calculations (PDF)

Crystallographic data of **1** (CIF)

AUTHOR INFORMATION

Corresponding Author

*E-mail: mitsudo@cc.okayama-u.ac.jp

*E-mail: suga@cc.okayama-u.ac.jp

Notes

The authors declare no competing financial interest.

ACKNOWLEDGMENT

This work was supported in part by a Grant-in-Aid for Scientific Research (C) (No. 16K05695) from JSPS, Japan and by JST, ACT-C, Japan.

REFERENCES

(1) For reviews, see: (a) Takimiya, K.; Shinamura, S.; Osaka, I.; Miyazaki, E., Thienoacene-Based Organic Semiconductors. *Adv. Mater.* **2011,** *23*, 4347–4370. (b) Rasmussen, S. C.; Evenson, S. J. *Prog. Polym. Sci.* **2013**, *38*, 1773–1804. (c) Ohshita, J. *Macromol. Chem. Phys.* **2009,** *210*, 1360–1370. (d) Romero-Nieto, C.; Baumgartner, T. *Synlett* **2013**, *24*, 920–937.

(2) (a) Karminski-Zamola, G. M.; Malesevic, M.; Bajic, M.; Golja, G. *Croat. Chem. Acta* **1992,** *65*, 847–849. (b) Kozmik, V.; Poznik, M.; Svoboda, J.; Frere, P. *Tetrahedron Lett.* **2015,** *56*, 6251–6253.

(3) (a) Wang, M.; Wei, J.; Fan, Q.; Jiang, X. *Chem. Commun.* **2017,** *53*, 2918–2921. (b) Youn, J.; Kewalramani, S.; Emery, J. D.; Shi, Y.; Zhang, S.; Chang, H.-C.; Liang, Y.-j.; Yeh, C.-M.; Feng, C.-Y.; Huang, H.; Stern, C.; Chen, L.-H.; Ho, J.-C.; Chen, M.-C.; Bedzyk, M. J.; Facchetti, A.; Marks, T. J. *Adv. Funct. Mater.* **2013,** *23*, 3850–3865. (c) Kang, I.; Park, S. M.; Lee, D. H.; Han, S.-H.; Chung, D. S.; Kim, Y.-H.; Kwon, S.-K. *Sci. Adv. Mater.* **2013,** *5*, 199–208. (d) Tian, H.; Han, Y.; Bao, C.; Yan, D.; Geng, Y.; Wang, F. *Chem. Commun.* **2012,** *48*, 3557–3559. (e) Huang, P.-Y.; Chen, L.-H.; Kim, C.; Hsiu-Chieh, C.; Liang, Y.-j.; Feng, C.-Y.; Yeh, C.-M.; Ho, J.-C.; Lee, C.-C.; Chen, M.-C. *ACS Appl. Mater. Interfaces* **2012,** *4*, 6992–6998. (f) Youn, J.; Chen, M.-C.; Liang, Y.-j.; Huang, H.; Ortiz, R. P.; Kim, C.; Stern, C.; Hu, T.-S.; Chen, L.-H.; Yan, J.-Y.; Facchetti, A.; Marks, T. J. *Chem. Mater.* **2010,** *22*, 5031–5041.

(4) (a) Mitsudo, K.; Shimohara, S.; Mizoguchi, J.; Mandai, H.; Suga, S. *Org. Lett.* **2012,** *14*, 2702–2705. (b) Mitsudo, K.; Sato, H.; Yamasaki, A.; Kamimoto, N.; Goto, J.; Mandai, H.; Suga, S. *Org. Lett.* **2015,** *17*, 4858–4861. (c) Kamimoto, N.; Schollmeyer, D.; Mitsudo, K.; Suga, S.; Waldvogel, S. R. *Chem. - Eur. J.* **2015,** *21*, 8257–8261. (d). Mitsudo, K.; Murakami, T.; Shibasaki, T.; Inada, T.; Mandai, H.; Ota, H.; Suga, S. *Synlett* **2016,** *27*, 2327–2332.

(5) (a) Saito, K.; Chikkade, P. K.; Kanai, M.; Kuninobu, Y. *Chem. - Eur. J.* **2015,** *21*, 8365–8368. (b) Kaida, H.; Satoh, T.; Hirano, K.; Miura, M. *Chem. Lett.* **2015,** *44*, 1125–1127.

(6) Marchand, G.; Decroix, B.; Morel, J. *J. Heterocycl. Chem.* **1984**, *21*, 877–880.

(7) McNab, H.; Hunter, G. A. *New. J. Chem.* **2010**, *34*, 2558–2563.

(8) Zhang, F.; Mitchell, D.; Pollock, P.; Zhang, T. Y. *Tetrahedron Lett.* **2007,** *48*, 2349–2352.

(9) Itami, K.; Yamaguchi, J.; Yamaguchi, A.; Mandal, D. *J. Am. Chem. Soc.* **2011**, *133*, 19660–19663.

(10) The structure of **1** was confirmed by X-ray crystallography: see the Supporting Information.

(11) For recent studies on the role of Ag salt in Pd-catalyzed C–H functionalizations, see: (a) Lee, S. Y.; Hartwig, J. F. *J. Am. Chem. Soc.* **2016,** *138*, 15278–15284. (b) Lotz, M. D.; Camasso, N. M.; Canty, A. J.; S., S. M. *Organometallics* **2017,** *36*, 165–171.

(12) The data of DFT calculations are described in the Supporting Information.

(13) For the details of cyclic voltammetry: see the Supporting Information.

(14) Pommerehne, J.; Vestweber, H.; Guss, W.; Mahrt, R. F.; Bässler, H.; Porsch, M.; Daub, J. *Adv. Mater.* **1995**, *7*, 551–554.

To format double-column figures, schemes, charts, and tables, use the following instructions:

Place the insertion point where you want to change the number of columns
From the **Insert** menu, choose **Break**
Under **Sections**, choose **Continuous**
Make sure the insertion point is in the new section. From the **Format** menu, choose **Columns**
In the **Number of Columns** box, type **1**
Choose the **OK** button

Now your page is set up so that figures, schemes, charts, and tables can span two columns. These must appear at the top of the page. Be sure to add another section break after the table and change it back to two columns with a spacing of 0.33 in.

Table 1. Example of a Double-Column Table

Column 1	Column 2	Column 3	Column 4	Column 5	Column 6	Column 7	Column 8

Authors are required to submit a graphic entry for the Table of Contents (TOC) that, in conjunction with the manuscript title, should give the reader a representative idea of one of the following: A key structure, reaction, equation, concept, or theorem, etc., that is discussed in the manuscript. Consult the journal's Instructions for Authors for TOC graphic specifications.